

02.73.16

Reprinted from:

2.B:2.G

Not to be reproduced by photoprint or microfilm without written permission from the publi

THE (d, <sup>6</sup>Li) REACTION ON <sup>64,66,68</sup>Zn ISOTOPES AT 27.25 MeV

A. E. CEBALLOS, H. J. ERRAMUSPE†, A. M. J. FERRERO, M. J. SAMETBAND†,  
J. E. TESTONI†, D. R. BÈS† and E. E. MAQUEDA†  
*Comisión Nacional de Energía Atómica, Departamento de Física Nuclear,  
Avda. Libertador 8250, Buenos Aires, Argentina*

Received 22 January 1973  
(Revised 19 March 1973)

Abstract: The differential cross sections for the reactions <sup>64,66,68</sup>Zn(d, <sup>6</sup>Li)<sup>60,62,64</sup>Ni lead-

C. N. E. A. Biblioteca	
ARCHIVO PUBLICACIONES	
NO 1	AÑO 1973



## THE (d, ${}^6\text{Li}$ ) REACTION ON ${}^{64,66,68}\text{Zn}$ ISOTOPES AT 27.25 MeV

A. E. CEBALLOS, H. J. ERRAMUSPE †, A. M. J. FERRERO, M. J. SAMETBAND †,  
 J. E. TESTONI †, D. R. BÈS † and E. E. MAQUEDA †

*Comisión Nacional de Energía Atómica, Departamento de Física Nuclear,  
 Avda. Libertador 8250, Buenos Aires, Argentina*

Received 22 January 1973

(Revised 19 March 1973)

**Abstract:** The differential cross sections for the reactions  ${}^{64,66,68}\text{Zn}(d, {}^6\text{Li}){}^{60,62,64}\text{Ni}$  leading to the ground  $0^+$  and the first  $2^+$  excited states of the residual nuclei are measured at 27.25 MeV. A DWBA analysis is performed using both phenomenological and microscopic form factors. The latter are calculated on the basis of the BCS plus RPA description of the initial and final nuclear states.

E NUCLEAR REACTIONS  ${}^{64,66,68}\text{Zn}(d, {}^6\text{Li})$ ,  $E = 27.25$  MeV; measured  $\sigma(\theta)$ .  
 ${}^{60,62,64}\text{Ni}$  levels deduced relative  $S$ . Enriched targets.

### 1. Introduction

Several papers <sup>1–6</sup>) on the (d,  ${}^6\text{Li}$ ) reaction in light nuclei have emphasized the direct character of the  $\alpha$ -particle transfer. In this paper we discuss the (d,  ${}^6\text{Li}$ ) reactions induced by 27.25 MeV deuterons in the isotopes  ${}^{64,66,68}\text{Zn}$ . In these medium mass nuclei the results also suggest a direct mechanism and, on this basis, we undertake an analysis of the data.

In sect. 2, we describe the experimental set-up. In sect. 3 we carry out a study of a typical spectrum showing the main features of the experimental results. In sect. 4 a DWBA analysis of the angular distributions of the cross sections is performed using a phenomenological form factor. In sect. 5, we apply the formalism of Dragún *et al.* <sup>7</sup>) to the microscopic calculation of the form factors. We include four-particle structure factors calculated on the basis of a BCS plus RPA description of the initial and final nuclei. Finally, in sect. 6, we present our conclusions on four-particle transfer reactions in the medium mass region.

### 2. Experimental method

The (d,  ${}^6\text{Li}$ ) reactions were investigated by bombarding self-supporting metallic foils with the external 27.25 MeV deuteron beam of the Buenos Aires 180 cm Synchrocyclotron. In order to reduce the neutron background in the experimental area, two

† Fellow of the Consejo Nacional de Investigaciones Científicas y Técnicas.

carbon collimators are located at about 7 m from the target, at the exit of the vacuum tank built for the modified regenerative system<sup>8</sup>). At the second defining slit, the beam has an emittance of  $50 \text{ mrad} \cdot \text{mm}$  both in the horizontal and vertical planes, with an energy spread of 300 keV for an intensity ranging from 1 nA to 20 nA. The beam passes through a first double quadrupole focusing lens, is bent by a  $37^\circ$  magnet and, finally, a second doublet allows a correct centering in the scattering chamber. The zero direction is determined to an accuracy of the order of  $0.1^\circ$ . The beam spot on the target is  $10 \times 4 \text{ mm}^2$ .

Two independent  $E$ - $\Delta E$  detector telescopes, operating simultaneously and placed in a symmetrical arrangement off the azimuthal plane, are mounted on a moving plate whose position can be determined to within  $0.05^\circ$  relative to the zero direction. The telescopes consist of two sets of  $(100\text{-}50) \mu\text{m}$  and  $(90\text{-}55) \mu\text{m}$  fully depleted surface-barrier Si detectors, with an energy resolution of 30 keV for 5.4 MeV  $\alpha$ -particles. They allow the  ${}^6\text{Li}$  particles to be completely stopped, whereas the lighter products of the reaction and the involved pile-up are well identified or do not interfere significantly with the levels studied. The overall energy resolution is 400 keV FWHM.

The electronic set-up consists of two conventional chains functionally identical. The events are registered in a 4096-channel Inter technique analyzer working in a  $64 \times 64$  bidimensional mode.

The targets used in this experiment were self-supporting foils of  ${}^{68}\text{Zn}$  (98.5%),  ${}^{66}\text{Zn}$  (96.8%) and  ${}^{64}\text{Zn}$  (99.1%) with thicknesses of  $1.1 \text{ mg} \cdot \text{cm}^{-2}$ ,  $1.1 \text{ mg} \cdot \text{cm}^{-2}$  and  $0.78 \text{ mg} \cdot \text{cm}^{-2}$ , respectively.

### 3. Experimental results

As a typical example, fig. 1 shows the spectrum of  ${}^6\text{Li}$  ions produced in the  ${}^{64}\text{Zn}(\text{d}, {}^6\text{Li}){}^{60}\text{Ni}$  reaction at  $30^\circ$  in the lab system. The  $0^+$  ground state level and the 1.33 MeV  $2^+$  level of the residual nucleus are clearly resolved. Because of the  $Q$ -value the  ${}^{59}\text{Ni}$  states populated in the  ${}^{64}\text{Zn}(\text{d}, {}^7\text{Li}){}^{59}\text{Ni}$  reaction are at least 4.13 MeV below the  $0^+$  ground state of  ${}^{60}\text{Ni}$ . Similar kinematic effects occur in almost all nuclei in the medium mass region, allowing the separation of the lowest states of the corresponding isotopes.

Figs. 2 and 3 show the differential cross sections corresponding to the  $0^+$  ground states and the lowest  $2^+$  states of the residual nuclei for the reactions  ${}^{64, 66, 68}\text{Zn}(\text{d}, {}^6\text{Li}){}^{60, 62, 64}\text{Ni}$ . The data are given in the c.m. system.

All the differential cross section angular distributions present a quite similar pattern for the three isotopes. They show the diffraction structure and forward peaking characteristics of a direct reaction mechanism. This fact may be simply expected by the small probability of  ${}^6\text{Li}$  emission in a compound nucleus reaction.

The magnitudes of the measured cross sections range approximately between  $1 \mu\text{b}$  and  $20 \mu\text{b}$  for the  $0^+$  state, the higher values corresponding to the lower mass number. They are consistent with the results reported for lighter nuclei, and in particular with

those obtained <sup>1)</sup> on Ca targets at 19.5 MeV. A DWBA calculation indicates that the  $\text{Zn}(d, {}^6\text{Li})\text{Ni}$  cross sections are about the same for an incident energy of 19.5 MeV, in spite of the fact that the Li ions are emitted with an energy corresponding to about the Coulomb barrier height.

The ratios between the intensities of the  $0^+$  and  $2^+$  levels are roughly conserved in the  ${}^{64,66,68}\text{Zn}$  isotopes.

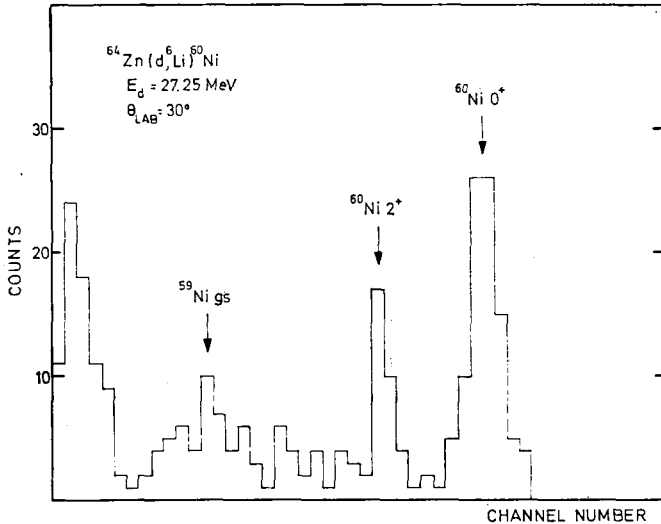


Fig. 1. The spectrum of Li ions obtained in reactions on  ${}^{64}\text{Zn}$  induced by 27.25 MeV deuterons, as observed in one of the detector systems at  $\theta_{\text{lab}} = 30^\circ$ .

#### 4. DWBA analysis

Calculations based on DWBA are carried out in order to verify the direct character of the reaction and to check the parentage between the target and final nuclei. It is assumed that the transferred  $\alpha$ -particle is a point ( $m = 4$ ) mass. Thus, we may construct a phenomenological form factor using the wave function of an  $\alpha$ -particle moving in a Woods-Saxon potential of radius, diffuseness and depth such that the  $\alpha$ -particle has the correct binding energy (see table 1). In the analysis described in this section we have used the radial quantum numbers  $N = 5$  and  $N = 4$  for  $L = 0$  and  $L = 2$  respectively, as suggested in ref. <sup>7)</sup>, and in the more exact calculation of sect. 5. The optical parameters for the deuteron channel are taken from ref. <sup>9)</sup>. The Li parameters are chosen within reasonable ranges in order to yield good agreement with experimental data. Both sets of optical parameters are shown in table 1. Only the real potential  $V$  presents some variation with the mass of the target. The Coulomb radius is large in the outgoing channel, as a consequence of the finite size of the Li ions.

In order to check the validity of the structure factors extracted from the experimental data, an extensive survey of the influence of the different Li optical parameters

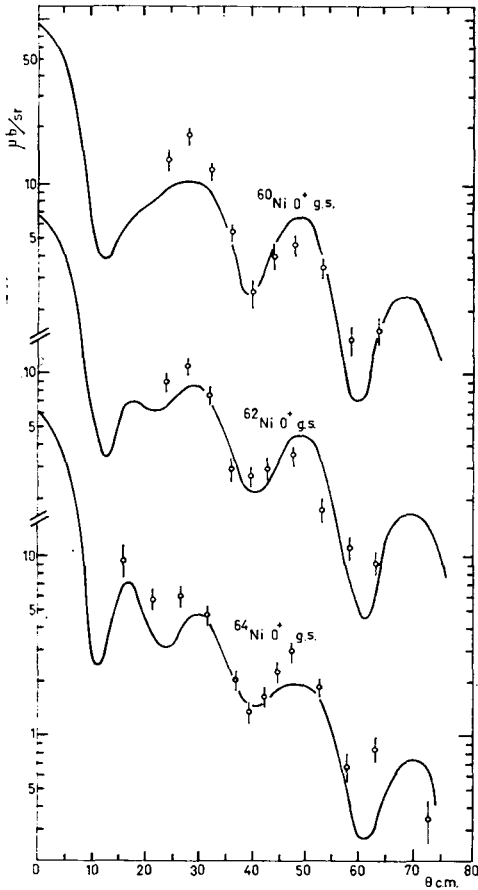


Fig. 2. The differential cross sections of the reactions  $^{64,66,68}\text{Zn}(d, ^6\text{Li})^{60,62,64}\text{Ni}$ , leading to the  $0^+$  ground state at  $E_d = 27.25$  MeV. The solid lines represent the DWBA calculations. A unique overall normalization factor is used both for these reactions and the ones shown in fig. 3.

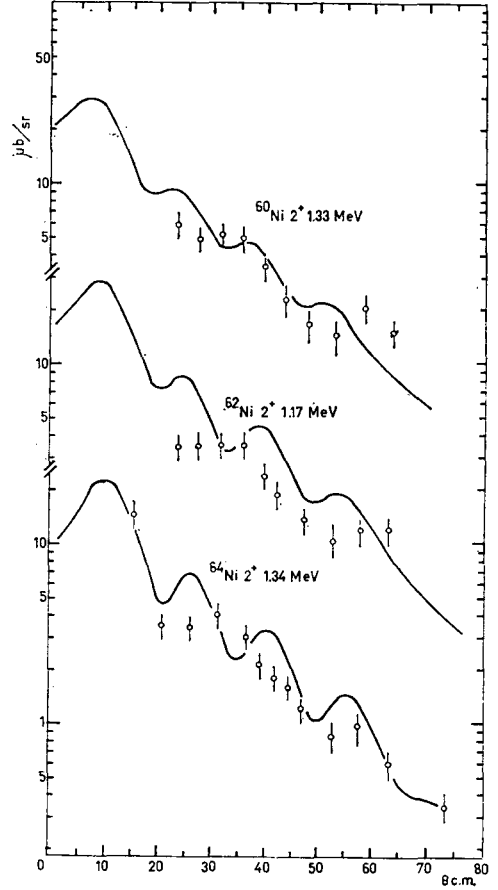


Fig. 3. The differential cross sections of the reactions  $^{64,66,68}\text{Zn}(d, ^6\text{Li})^{60,62,64}\text{Ni}$ , leading to the  $2^+$  first excited state at  $E_d = 27.25$  MeV. Solid lines represent the DWBA calculations. A unique overall normalization factor is used both for these reactions and the ones shown in fig. 2.

has been performed. Changes of about 20% in the dispersive potential  $V$ , in the derivative absorptive potential  $W$ , in the radius  $R_W = r_{0W}A^{\frac{1}{3}}$  and the diffuseness  $a_W$  of the imaginary potential, and in the Coulomb radius  $R_C = r_{0C}A^{\frac{1}{3}}$ , have relatively little effect on the magnitudes of the differential cross sections, in spite of important changes in their shapes. On the other hand, variations of the same order of magnitude in the radius  $R_V = r_{0V}A^{\frac{1}{3}}$  and in the diffuseness  $a_V$  of the real potential, affect the absolute magnitude of the cross sections. However, the relative strengths of the  $0^+$  and  $2^+$  levels are conserved.

The dependence of the shapes of the differential cross sections on the number of nodes  $N$  was also investigated. No substantial changes are observed in the range from

$N = 0$  to  $N = 6$ , neither in the shape of the differential cross sections nor in the relative magnitude.

We may construct in a similar way the phenomenological form factors for the three isotopes. Only the potential well depth is varied in order to yield the correct binding energy in each case. In particular, using the same arbitrary normalization for the

TABLE 1

The optical parameters for the deuteron and lithium channels and the parameters for the bound  $\alpha$ -particle well

	Deuteron channel	Lithium channel	$\alpha$ -particle well
$V$ (MeV)	71.9	335 for ${}^{64}\text{Zn}$ 317 for ${}^{66}\text{Zn}$ 310 for ${}^{68}\text{Zn}$	adjusted to get the binding energy
$W$ (MeV)	56	75	
$r_{0V}$ (fm)	0.96	1.50	1.25
$a_V$ (fm)	0.99	0.65	0.65
$r_{0W}$ (fm)	1.35	1.50	
$a_W$ (fm)	0.75	0.65	
$r_{0C}$ (fm)	1.25	2.50	1.25
$a_C$ (fm)	0.00	0.00	0.00

TABLE 2

The relative cross sections for the three target isotopes

Target nucleus	$0^+$		$2^+$	
	$\frac{(d\sigma/d\Omega)_{\text{exp.}}}{(d\sigma/d\Omega)_{\text{phen.}}}$	$\frac{(d\sigma/d\Omega)_{\text{mic.}}}{(d\sigma/d\Omega)_{\text{phen.}}}$	$\frac{(d\sigma/d\Omega)_{\text{exp.}}}{(d\sigma/d\Omega)_{\text{phen.}}}$	$\frac{(d\sigma/d\Omega)_{\text{mic.}}}{(d\sigma/d\Omega)_{\text{phen.}}}$
${}^{64}\text{Zn}$	1.00	1.00	1.00	1.00
${}^{66}\text{Zn}$	0.83	0.90	1.27	1.26
${}^{68}\text{Zn}$	0.79	0.71	1.38	1.40

The second and fourth columns contain the relative ratios of the experimental cross sections and the cross sections obtained with the phenomenological form factors of sect. 4. The third and fifth columns include analogous expressions with the experimental cross sections replaced by the microscopic ones of sect. 5. The results are obtained from the best fits of the corresponding angular distributions in which the only variable parameter is the normalization factor.

three isotopes, the ratio of the experimental to the DWBA cross sections gives a relative spectroscopic factor in which the effects associated with the reaction mechanism are eliminated (see table 2). It is apparent that these relative spectroscopic factors decrease with  $A$  for the reactions populating the ground state and increase for the reactions leading to the  $2^+$  state.

### 5. Microscopic construction of the form factor

We analyze the magnitudes of the cross sections for the  $0^+$  and  $2^+$  final states of the reactions  ${}^{64, 66, 68}\text{Zn}(d, {}^6\text{Li}){}^{60, 62, 64}\text{Ni}$ , following the formalism proposed by Dragún *et al.* <sup>7)</sup>.

The differential cross sections can be written as a coherent sum over the radial quantum number  $N$ :

$$\frac{d\sigma}{d\Omega} \propto \sum_{L, M} (2L+1) \left| \sum_N G_{NL} B_{NL}^M \right|^2, \quad (1)$$

where  $N$ ,  $L$  and  $M$  are the radial quantum number, orbital angular momentum and magnetic quantum number of the transferred cluster. The kinematic factors  $B_{NL}^M$  represent the probability amplitude for transferring a point  $m = 4$  particle into the orbital state labeled by  $N$  and  $L$  of a structureless nucleus. They are computed with a DWUCK code <sup>10)</sup>.

The nuclear structure factors  $G_{NL}$ , are related to the probability of finding, in the target nucleus, an  $\alpha$ -particle with quantum numbers  $N$  and  $L$ .

They include:

- (a) Center-of-mass and angular momentum transformation coefficients.
- (b) The overlap integrals between the relative wave functions of the transferred particles moving in the fields of the final nucleus and in the  ${}^6\text{Li}$  ion respectively. The nuclear oscillator parameter  $\nu = 0.99 A^{-3/2} \text{fm}^{-2}$  and the size parameter for the  ${}^6\text{Li}$   $\eta = 0.6 \text{fm}^{-2}$  were used in the computation of these overlap integrals.
- (c) The spectroscopic amplitudes, which are given by

$$C_{T_f J_f}^{J_i T_i}(j_1 j_2 j_3 j_4 J_{12} J_{34} T_{12} L) = \frac{\langle \Psi_{A+4}(J_i T_i) || T_{LM}^+ || \Psi_A(T_f J_f) \rangle}{\sqrt{(2J_i+1)(2T_i+1)}}. \quad (2)$$

The reduced matrix elements of the four-particle operator  $T_{LM}^+$ , coupled to the angular momentum  $L$  and isotopic spin  $T = 0$ , are calculated between the states of the target and residual nuclei.

In the above formalism we do not make the approximation that the size parameters in the  ${}^6\text{Li}$  and in the target nuclei are the same, with the consequent contribution of only one  $G_{NL}$  factor. This may be valid for the analysis of  $(d, {}^6\text{Li})$  reactions in light nuclei <sup>1)</sup> but, in our case, the coherent contributions of several  $G_{NL}$  factors are needed for a more accurate calculation of the cross sections.

In order to evaluate  $C_{T_f J_f}^{J_i T_i}$  we assume that the  ${}^4\text{Zn}$  initial state is given by a product wave function where the two protons are coupled to zero angular momentum and the valence neutrons are represented by the same BCS ground state solution as in the  ${}^{A-2}\text{Ni}$  nucleus:

$$|{}^4\text{Zn, g.s.}\rangle = \sqrt{\frac{1}{2}} \sum_j \lambda_j (b_j^+ b_j^+)_{0-1}^0 |\text{BCS, } {}^{A-2}\text{Ni}\rangle. \quad (3)$$

The coefficients  $\lambda_j$  measure the distribution of the two protons among the different  $j$ -subshells. The symbol  $(b_j^+ b_j^+)_{m_i m_t}^{l t}$  denotes the coupling of the particle creation operators  $b_j^+$  to the angular momentum  $l$ , with projection  $m_l$  and isospin  $t$ , with projection  $m_t$ .

The final ground and excited states of the Ni isotopes are described in terms of the pairing-plus-quadrupole model, which are treated within the BCS and RPA approximations<sup>12, 13</sup>).

The present description of the initial and final states selects those components of the four-body transfer operator  $T_{LM}^+$  in which the two protons are coupled to zero angular momentum:

$$T_{LM}^+(j_1 j_2 j_3 j_4) = \delta(j_3 j_4) \Omega \{ (b_{j_3}^+ b_{j_4}^+)^{01} (b_{j_1}^+ b_{j_2}^+)^{L1} \}_{M0}^{L0}, \quad (4)$$

where

$$\Omega = \sqrt{\frac{1}{2}} \left\{ 1 + \delta(j_1 j_2) (-)^L + \frac{\delta(j_1 j_3) + \delta(j_2 j_3)}{2j_3 + 1} + \delta(j_1 j_3) \delta(j_2 j_3) \left( \delta(L0) + \frac{(-)^L}{2j_3 + 1} \right) \right\}^{-\frac{1}{2}} \quad (5)$$

is the factor required in order that  $T_{LM}^+(j_1 j_2 j_3 j_4)$  acting in the vacuum state yields a normalized wave function. Within these assumptions, the matrix elements corresponding to the transfer operators are:

$$\begin{aligned} \langle \text{Ni}, 0^+ | T_0(j_1 j_2 j_3 j_4) | \text{Zn}, 0^+ \rangle &= \Omega \sqrt{\frac{1}{3}} \lambda_{j_3} (-)^{l_1} \sqrt{2j_1 + 1} U_{j_1} V_{j_1}, \quad (6) \\ \langle \text{Ni}, 2^+ | T_2(j_1 j_2 j_3 j_4) | \text{Zn}, 0^+ \rangle &= \Omega A \sqrt{\frac{1}{3}} \lambda_{j_3} (-)^{l_1} \langle j_1 || r^2 Y_2 || j_2 \rangle \\ &\quad \times (U_{j_1} V_{j_2} + U_{j_2} V_{j_1}) \left\{ \frac{V_{j_1} V_{j_2}}{E_{j_1} + E_{j_2} - \omega} + \frac{U_{j_1} U_{j_2}}{E_{j_1} + E_{j_2} + \omega} \right\}, \end{aligned}$$

where  $U_j$  and  $V_j$  are the well-known coefficients of the Bogolyubov-Valatin transformation. The factor  $A$  is the normalization constant in the RPA formulation; the term  $\langle j_1 || r^2 Y_2 || j_2 \rangle$  is the reduced matrix element of the quadrupole operator; the  $E_j$  are the quasiparticle energies and  $\omega$  is the phonon energy, which is assumed to be the empirical energy of the  $2^+$  state.

From ref.<sup>11</sup>) we use the values  $\lambda_p = 0.78$ ,  $\lambda_f = 0.55$  and  $\lambda_n = 0.31$ . The BCS problem for the different isotopes has been resolved by taking a pairing strength  $G = 0.346$  MeV which is deduced from the energy gap  $\Delta = 1.50$  MeV as in ref.<sup>12</sup>) for  ${}^{62}\text{Ni}$ . In the calculations we have included the  $f_{\frac{3}{2}}$ ,  $p_{\frac{3}{2}}$ ,  $f_{\frac{5}{2}}$ ,  $p_{\frac{5}{2}}$ ,  $g_{\frac{3}{2}}$ ,  $g_{\frac{5}{2}}$  and  $d_{\frac{3}{2}}$  shells; the corresponding single-particle energies,  $\varepsilon_j$ , are given in table 3. This microscopic calculation of the  $T_{LM}^+$  operator includes the contributions of a more detailed set of configurations than has been used in the analysis of similar reactions in lighter nuclei [ref.<sup>1</sup>)].

Solid lines in figs. 2 and 3 correspond to the results of the calculations. A unique overall normalization is used for the six angular distributions. As is shown in sect. 4,

the ground state cross sections corresponding to the different isotopes decrease as the mass number increases. This effect is only partly due to the kinematics of a DWBA calculation; the introduction of the structure information through the  $G_{NL}$  coefficients is needed in order to obtain the quantitative agreement shown in figs. 2 and 3 and in table 2.

The mass dependence of the cross sections can be explained by the progressive filling of the  $p_{\frac{3}{2}}$  shell. As it is well known<sup>14</sup>), the probability of a relative s-state is larger for a  $(p)^2$  configuration than for an  $(f)^2$  configuration and the probability of finding a particle outside the nuclear radius is somewhat larger in a state with two

TABLE 3  
The single-particle energies for the shells included in the BCS calculations

$j$	$\epsilon_j$ (MeV)
$f_{\frac{7}{2}}$	-4.00
$p_{\frac{3}{2}}$	0.00
$f_{\frac{5}{2}}$	0.75
$p_{\frac{1}{2}}$	1.05
$g_{\frac{7}{2}}$	4.95
$g_{\frac{9}{2}}$	9.57
$d_{\frac{5}{2}}$	9.57

radial nodes than in a single-node state. Both effects favour the spectroscopic amplitudes involving  $(2p_{\frac{3}{2}})^2$  pairs over those corresponding to  $(1f_{\frac{3}{2}})^2$  pairs. Therefore, the ground state cross section should decrease as the factor  $U_{\frac{3}{2}}V_{\frac{3}{2}}$  decreases and the factor  $U_{\frac{5}{2}}V_{\frac{5}{2}}$  increases, or, in other words, as the  $2p_{\frac{3}{2}}$  orbit becomes completely occupied.

## 6. Conclusions

The yields of the  $(d, {}^6\text{Li})$  reactions performed in medium mass nuclei for energies of the outgoing particles not too much over the Coulomb barrier are comparable with those obtained in the case of light nuclei<sup>1</sup>).

From the phenomenological analysis we conclude:

(a) The shapes of the cross sections are in good agreement with the calculations based on the hypothesis of a direct interaction mechanism. However this statement is influenced by the fact that we start measuring only at about  $20^\circ$  and therefore we are not able to verify the existence of the strong forward peaking expected from DWBA.

(b) The detailed shape of the form factor is not important in the present case, provided they have the appropriate tail. In particular, the assumption of a  $m = 4$   $\alpha$ -particle which is bound in the potential well of the residual nucleus provides a good form factor for the description of four-particle pick-up reactions induced by deuterons in this range of energies.

(c) The relative strength of the  $0^+$  and  $2^+$  states can be determined within an error of 20 %, taking into consideration the sensitivity of the present DWBA calculations to the optical parameters.

Finally, in order to obtain the form factor corresponding to an  $\alpha$ -particle transfer, we have used the formalism that includes structure factors calculated on the basis of the pairing-plus-quadrupole model. These calculations give a very good and coherent picture of the relative magnitudes of the cross sections for the different isotopes, both in the  $0^+$  ground and  $2^+$  first excited states.

We would like to thank Drs. G. G. Dussel and R. P. J. Perazzo for many illuminating discussions and stimulating suggestions.

### References

- 1) H. Gutbrod, H. Yoshida and R. Bock, Nucl. Phys. **A165** (1971) 240
- 2) L. J. Denes and W. Daenick, Phys. Rev. **154** (1967) 928
- 3) J. B. Gerhard, P. Mizera and F. W. Slec, Annual report, Univ. of Washington, 1964
- 4) A. Ceballos, H. Erramuspe, A. Ferrero, M. Sametband and J. Testoni, Phys. Rev. **C4** (1971) 1959
- 5) W. Eichelberger, R. D. Plieninger and E. Velten, Nucl. Phys. **A149** (1970) 441
- 6) H. Gutbrod, H. Yoshida and R. Bock, Proc. Int. Conf. on nuclear reactions induced by heavy ions, Heidelberg 1969 (North-Holland, Amsterdam, 1970) p. 311
- 7) O. Dragun, G. Dussel, E. Maqueda and R. Perazzo, Nucl. Phys. **A167** (1971) 529
- 8) S. Mayo and M. Sametband, Nucl. Instr. **60** (1968) 261
- 9) P. E. Hodgson, Adv. in Physics, Phil. Mag. Suppl. **15** (1966) 329
- 10) P. D. Kunz, University of Colorado, report C00-535-606, unpublished
- 11) R. P. Perazzo, Nucl. Phys. **A186** (1972) 379; and private communication
- 12) L. S. Kisslinger and R. Sorensen, Rev. Mod. Phys. **35** (1963) 910
- 13) D. R. Bès and R. Sorensen, Adv. in Nucl. Phys., vol. 2 (Plenum Press, 1969) p. 129
- 14) B. Bayman and N. Hintz, Phys. Rev. **172** (1968) 1113